The predicted infrared spectrum of the hypermetallic molecule CaOCa in its lowest two electronic states X~1Σg+ and a˜3Σu+

ARTICLE *in* JOURNAL OF MOLECULAR STRUCTURE · SEPTEMBER 2012

Impact Factor: 1.6 · DOI: 10.1016/j.molstruc.2012.03.048

Journal of Molecular Structure 1023 (2012) 101–107

Contents lists available at SciVerse ScienceDirect

Journal of Molecular Structure

journal homepage: www.elsevier.com/locate/molstruc

The predicted infrared spectrum of the hypermetallic molecule CaOCa in its lowest two electronic states $\widetilde{X}^1\Sigma_g^+$ and $\tilde{a}^3\Sigma_u^+$ ☆

B. Ostojić [a], P.R. Bunker [b,*], P. Schwerdtfeger [b,c], Artur Gertych [d], Per Jensen [b,d]

[a] Institute of Chemistry, Technology and Metallurgy, University of Belgrade, Studentski trg 14-16, 11000 Belgrade, Serbia
[b] Centre for Theoretical Chemistry and Physics (CTCP), The New Zealand Institute for Advanced Study (NZIAS), Massey University Auckland, Private Bag 102904, North Shore City, 0745 Auckland, New Zealand
[c] Fachbereich Chemie, Philipps-Universität Marburg, Hans-Meerwein-Str., D-35032 Marburg, Germany
[d] FB C – Physikalische und Theoretische Chemie, Bergische Universität, D-42097 Wuppertal, Germany

ARTICLE INFO

Article history:
Received 18 February 2012
Received in revised form 14 March 2012
Accepted 22 March 2012
Available online 30 March 2012

Keywords:
CaOCa
Ab initio 3D potential energy surfaces
Rovibronic spectra

ABSTRACT

This study of CaOCa is our third paper in a series on Group 2 alkaline-earth M_2O hypermetallic oxides. As with our previous calculations for BeOBe and MgOMg, the *ab initio* calculations we report here show that CaOCa has a linear $^1\Sigma_g^+$ ground electronic state and a very low lying linear $\tilde{a}^3\Sigma_u^+$ first excited triplet electronic state. For CaOCa we determine that the singlet–triplet splitting $T_e(\tilde{a}) = 386\ cm^{-1}$. We calculate the three-dimensional potential energy surface, and the electric dipole moment surfaces, of each of the two states using a multireference configuration interaction (MRCISD) approach in combination with internally contracted multireference perturbation theory (RS2C) based on full-valence complete active space self-consistent field (FV-CASSCF) wavefunctions with a cc-pwCVQZ-DK basis set for Ca and a cc-pCVQZ basis set for O. We simulate the infrared absorption spectra of $^{40}Ca^{16}O^{40}Ca$ in each of these electronic states in order to aid in its eventual spectroscopic characterization.

1. Introduction

The elucidation of the stability and structure of metal-rich clusters is an important field of study, particularly as it impacts the development of new catalytic materials; both *ab initio* calculations and spectroscopic measurements play a crucial role in such work. Our contribution in this area is to make a detailed *ab initio* study of all of the Group 2 (alkaline earth) hypermetallic M_2O oxides. This requires us to carry out *ab initio* calculations of the full three-dimensional potential energy and dipole moment surfaces for the lowest electronic states, which we use to simulate the associated rovibronic absorption spectra. We have so far reported our results for Be_2O [1] and Mg_2O [2]. The present paper reports our results for Ca_2O, the next member.

Infrared spectra due to Ca_2O were assigned by Andrews and coworkers in their studies [3,4] of the products of the reaction of calcium metal with ozone, and with oxygen, in solid nitrogen at 15 K. The more recent of these two spectroscopic studies reports the results of reacting ^{44}Ca with $^{16}O_3$, and of reacting ^{40}Ca with $^{16}O_3$ and with $^{18}O_3$. The infrared spectra of the reaction products, in the 15 K nitrogen matrix, were recorded in the 400–800 cm^{-1} region. Two vibrational-transition peaks were attributed to symmetrical Ca_2O: At 486.8 and 476 cm^{-1} for $^{40}Ca_2{}^{16}O$; at 472 and 461 cm^{-1} for $^{40}Ca_2{}^{18}O$; and at 477 and 468 cm^{-1} for $^{44}Ca_2{}^{16}O$. Considering the isotopic shifts of the observed vibrational transitions (which were assumed to be associated with the symmetric Ca–O stretch, denoted ν_1 in contemporary notation [5]) it was concluded that the Ca_2O molecule that carries these peaks has the structure of an isosceles triangle with a CaOCa bond angle of approximately 120°. Peaks at 542.5, 526.5 and 533.5 cm^{-1} were assigned as being due to unsymmetrical $^{40}Ca^{40}Ca^{16}O$, $^{40}Ca^{40}Ca^{18}O$ and $^{44}Ca^{44}Ca^{16}O$, respectively. The calculations presented here do not support these identifications. Instead, we find that for CaOCa, as we found for BeOBe and MgOMg, the ground electronic state is a symmetrical linear $^1\Sigma_g^+$ state, and there is a very low lying $\tilde{a}^3\Sigma_u^+$ triplet electronic state. We note that for Group 2 difluorides, there was a debate for a long time over whether they were linear or bent [6,7]. Therefore, we calculate the three-dimensional potential energy and dipole moment surfaces of each of these states, and simulate their infrared absorption spectra, in the hope of encouraging the unambiguous identification of the spectrum of Ca_2O. We find that the strongest infrared absorptions, for both the singlet ground state and the low lying triplet state, are for the ν_3 asymmetric CaO stretching fundamental at 755 cm^{-1}.

The singlet–triplet splitting $T_e(\tilde{a})$ in these Group 2 M_2O molecules is of particular interest to us since for the heavier members

☆ This paper honors Professor Jaan Laane on the occasion of his 70th birthday.

* Corresponding author. Tel.: +1 613 990 0738; fax: +1 613 947 2838.
E-mail address: philip.bunker@nrc.ca (P.R. Bunker).

0022-2860/$ - see front matter © 2012 Published by Elsevier B.V.
http://dx.doi.org/10.1016/j.molstruc.2012.03.048

of the group, where relativistic effects are important, the weak singlet–triplet spectrum of such a molecule may be an appropriate target for investigating the possible time-variation of the fine structure constant α [8]. In the present work we have determined that for CaOCa, $T_e(\tilde{a}) = 386\ \mathrm{cm}^{-1}$. For BeOBe and MgOMg we calculated singlet–triplet splittings of 293 and 670 cm^{-1}, respectively. One of the aims of our future works on Sr_2O, Ba_2O and Ra_2O is to determine if they have close lying singlet and triplet states, one of which is the ground state.

CaO is the normally-stochiometric 'parent molecule' of Ca_2O and it has been the subject of considerable interest (see Refs. [9–11] and references therein). Since the fundamental band of CaO is in the region that we predict for the ν_3 fundamental of CaOCa, we also simulate the CaO fundamental band of CaO for comparison. In order to simulate the CaO fundamental with absolute intensities we make an *ab initio* calculation of the dipole moment of CaO over a range of relevant internuclear distances. We find that the ν_3 fundamental band of CaOCa, which we calculate to be at 755 cm^{-1}, has a much greater intrinsic intensity than the CaO fundamental band which is at about 720 cm^{-1}.

2. The *ab initio* calculation

2.1. Potential energy and dipole moment surfaces

As mentioned in the introduction, Andrews and Ault [4] concluded from their low-resolution spectra of matrix isolated calcium oxides that the CaOCa molecule exists in two isomers in a 15 K matrix: A symmetrical CaOCa bent isomer, and an unsymmetrical Ca-CaO isomer. In the present work, we initially investigated the question of the equilibrium geometry by performing a full geometry optimization. For these test calculations, we used a small active space, CAS(2,2), where the notation indicates that two electrons are distributed among two active orbitals, taken to be the two highest occupied molecular orbitals (HOMO). At the CAS(2,2)-MRCISD/6–311++G(2d,2p) level of theory, the ground electronic state of CaOCa has a linear symmetrical equilibrium geometry, and there are no local minima at bent geometries. The ground electronic state of the CaOCa molecule is found to be $\widetilde{X}^1\Sigma_g^+$, and the first excited electronic state is found to be a low-lying triplet state, $\tilde{a}^3\Sigma_u^+$, also with a linear symmetrical equilibrium geometry.

For our potential surface calculations leading to the simulation of the infrared spectra of the two states, the potential energy surfaces of the $\widetilde{X}$ and $\tilde{a}$ electronic states were computed using the complete active space (CASSCF) technique [12,13], followed by a multi-reference configuration interaction (MRCI) treatment [14–16] in conjunction with a modified version of CASPT2 (Complete Active Space with Second-order Perturbation Theory) developed by Celani and Werner [17] and referred to as RS2C. The basis set employed for the Ca atom was the Douglas-Kroll correlation consistent polarized core valence quadruple-zeta basis set of Koput and Peterson [18] (abbreviated as cc-pwCVQZ-DK in the text) which is required to account for the core-valence correlation of the 3s and 3p calcium orbitals. The O atom was described using the correlation-consistent polarized core-valence quadruple-zeta basis sets of Dunning et al. cc-pCVQZ [19] which was obtained by augmenting the standard cc-pVQZ basis sets with additional shells of tight functions (3s, 3p, 2d, 1f). This basis set was obtained from the EMSL database [20]. The basis set for CaOCa consists thus of 302 contracted functions. All electronic structure calculations were carried out using the MOLPRO 2008.1 suite of programs [21].

In contrast to the low-lying triplet state, the description of the $\widetilde{X}^1\Sigma_g^+$ ground electronic state of CaOCa requires a multiconfigurational representation. CASSCF calculations show that the two most important configurations of this state are $|1\sigma_g^2\ 1\sigma_u^2\ 2\sigma_g^2\ 2\sigma_u^2\ 3\sigma_g^2\ 3\sigma_u^2\ 4\sigma_g^2\ 1\pi_u^4\ 1\pi_g^4\ 5\sigma_g^2\ 4\sigma_u^2\ 6\sigma_g^2\ 2\pi_u^4\ 2\pi_g^4\ 5\sigma_u^2\ 7\sigma_g^2\ 6\sigma_u^2\ 3\pi_u^4\ 8\sigma_g^2\rangle$ and $|\ldots\ 3\pi_u^4\ 7\sigma_u^2\rangle$. At linearity, the coefficients in the CI expansion of these two dominant configurations are 0.74 and −0.60, respectively. The $\tilde{a}^3\Sigma_u^+$ state is well described by a single-reference wavefunction: $|\ldots\ 3\pi_u^4\ 8\sigma_g^1\ 7\sigma_u^1\rangle$ with a coefficient of 0.95 in the CI expansion at linearity. The stability and strong bonding character of the $\widetilde{X}$ and $\tilde{a}$ states arise from the predominantly ionic $Ca^+O^{2-}Ca^+$ nature of both states with the two separate electron spins of the Ca^+ ions, at opposite ends of the molecule, having little spin coupling. This lack of spin coupling explains the near-degeneracy of the $\widetilde{X}$ and $\tilde{a}$ states.

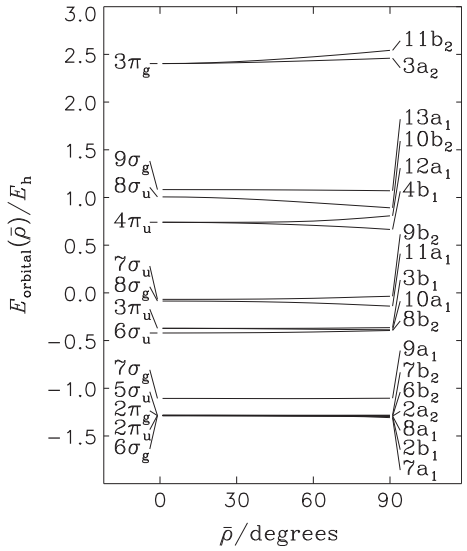

Fig. 1. The orbital energies of the pseudo-canonical orbitals of CaOCa as a function of $\bar{\rho} = 180^\circ - \angle(\mathrm{Ca{-}O{-}Ca})$ calculated with fixed Ca–O bond length in the framework of $\boldsymbol{C}_{2v}$ symmetry using full-valence CASSCF with a cc-pwCVQZ-DK basis set for Ca and a cc-pCVQZ basis set for O.

In Fig. 1 we plot the Walsh diagram [22] for the molecular orbitals. The orbital energies are plotted as functions of the bending angle. We take the orbital energies as those of the pseudo-canonical orbitals obtained from state-averaged full-valence CASSCF for the $\widetilde{X}$ and $\tilde{a}$ states using a cc-pwCVQZ-DK basis set for Ca and a cc-pCVQZ basis set for O. These energies were calculated with the Ca–O bond length fixed at its equilibrium value. The $7\sigma_g$ molecular orbital (MO) is the oxygen 2s orbital, the $6\sigma_u$ orbital is mainly oxygen $2p_z$ directed along the molecular axis, and the $3\pi_u$ orbital consists mainly of the oxygen $2p_{x,y}$ orbitals perpendicular to the molecular axis. The highest occupied MOs are $8\sigma_g$ and $7\sigma_u$. They are mainly symmetric and antisymmetric linear combinations, respectively, of the calcium 4s orbitals. The CASSCF active space used, denoted as CAS(10,12), consists of all configurations obtained by distributing the 10 valence electrons ($2s^2 2p^4$ on O and $4s^2$ on each Ca) in 12 MOs. In the framework of $\boldsymbol{C}_{2v}$ symmetry, the active space consists of five orbitals of A_1 symmetry ($9a_1$ to $13a_1$), two of B_1 symmetry ($3b_1$ and $4b_1$), four of B_2 symmetry ($8b_2$ to $11b_2$), and one of A_2 symmetry ($3a_2$); nine orbitals of A' symmetry ($16a'$ to $24a'$) and three of A'' symmetry ($5a''$ to $7a''$) in the $\boldsymbol{C}_s$ group. For the singlet and triplet electronic states we used the CASSCF state averaging (SA) procedure, i.e. 1^1A_1 and 1^3B_2 in the $\boldsymbol{C}_{2v}$ group ($1^1A'$ and $1^3A'$ in the $\boldsymbol{C}_s$ group), and the two states were included with equal weights. The CI expansion of the CASSCF wavefunction starting from the CAS(10,12) orbitals was generated within the internally contracted method with single and double substitutions (MRCISD) from each reference determinant. In these MRCISD calculations all ten valence electrons were correlated and the effect of higher excitations was taken into account through the Davidson

Table 1
The potential energy parameters of $\tilde{X}^1\Sigma_g^+$ and $\tilde{a}^3\Sigma_u^+$ CaOCa obtained by fitting the analytical function of Eq. (2) through the calculated *ab initio* energies.[a]

	$\tilde{X}^1\Sigma_g^+$	$\tilde{a}^3\Sigma_u^+$
r_{12}^e (Å)	1.99521(16)[b]	1.99883(14)
a_1 (Å^{-1})	2.0[c]	2.0
G_{000}[d]/(E_h)	−1435.039145(12)	−1435.0373860(98)
G_{001}	1119(44)	2590(34)
G_{002}	409(346)	1424(136)
G_{003}	−711(950)	5599(130)
G_{004}	1439(792)	
G_{101}	85(123)	−230(57)
G_{102}	3496(553)	−4624(91)
G_{103}	−6918(608)	
G_{200}	15778(66)	15807(58)
G_{201}	−1851(246)	−633(306)
G_{110}	2701(46)	2827(36)
G_{111}	−3236(824)	−664(363)
G_{112}	12378(1907)	
G_{300}	4710(135)	4699(119)
G_{210}	498(173)	502(143)
G_{400}	2751(647)	2905(578)

[a] Units are cm^{-1} unless otherwise indicated. For CaOCa, $r_{32}^e = r_{12}^e, a_3 = a_1$, and $G_{jkl} = G_{kjl}$.
[b] Quantities in parentheses are standard errors in units of the last digit given.
[c] Parameters, for which no standard error is given, were held fixed in the least squares fitting.
[d] G_{000} is the potential energy value at equilibrium.

correction [23] (henceforth we denote this full valence level of theory as FV-CAS(10,12)-MRCISD + Q and the energy resulting from it as E_{MRCI}).

To account for core-valence correlation, two types of RS2C calculations were performed, using the FV-CAS(10,12) wavefunctions as references. In the first type (resulting in an energy which we designate as $E_{RS2C}^{(1)}$), the electrons from the 3p orbitals of the calcium atoms are included in the correlation. Therefore, the core MOs $6\sigma_g$ and $5\sigma_u$ (which chiefly correspond to the symmetric and antisymmetric linear combinations, respectively, of the calcium $3p_z$ orbitals directed along the molecular axis) and the MOs $2\pi_u$ and $2\pi_g$ orbitals (which mainly consist of the symmetric and antisymmetric linear combinations, respectively, of the $3p_{x,y}$ calcium orbitals perpendicular to the molecular axis) are correlated in the RS2C approach. The $7a_1$ and $7b_2$ molecular orbitals correlate with the $6\sigma_g$ and $5\sigma_u$ species, respectively, at linear molecular geometries. Upon bending, the $2\pi_u$ orbital splits into the $8a_1$ and $2b_1$ orbitals whereas $2\pi_g$ splits into the $6b_2$ and $2a_2$. In the second type of RS2C calculations (resulting in an energy denoted as $E_{RS2C}^{(2)}$), the MOs corresponding to 3p atomic orbitals (AO) of Ca are kept frozen. To avoid intruder state problems we applied an energy shift of $0.1E_h$ and energies obtained in the RS2C calculations are corrected for this shift. The energy values for the construction of the potential energy surfaces were obtained as

$$E = E_{MRCI} + E_{RS2C}^{(1)} - E_{RS2C}^{(2)} \quad (1)$$

with the difference of the last two values accounting for core and core-valence correlation. This correction was necessary as the core polarizability of Ca^{2+}, 3.26 a.u., is already quite large within the Group 2 series of ions [24]. Scalar relativistic effects were taken into account by applying the second-order Douglas–Kroll–Hess Hamiltonian (DKH) [25–27] as incorporated in the MOLPRO 2008.1 program package.

The dipole moment surfaces for the two electronic states were obtained at the FV-CAS(10,12)-MRCISD level of theory in $\mathbf{C}_s$ point group symmetry.

The potential energy and dipole moment values were obtained at 77 unique geometries for the singlet state and 59 unique geometries for the triplet state with bond lengths between 1.86 Å and 2.15 Å and bond angles between 180° and 110°. The geometries were chosen such that for each of the two electronic states $\tilde{X}\ ^1\Sigma_g^+$ and $\tilde{a}^3\Sigma_u^+$, the energy range up to 1500 cm^{-1} above the respective minimum was covered for the subsequent rovibrational analysis. We choose this rather limited energy range because we aim at calculating accurately the lowest-lying rovibrational energy levels, in particular the fundamental energies, of Ca_2O. The spectra involving these energy levels are expected to provide the initial spectroscopic characterization of Ca_2O.

3. The morbid calculations

3.1. The rovibrational calculations

Having calculated the potential energy and dipole moment surfaces of the CaOCa molecule in its $\tilde{X}$ and $\tilde{a}$ states at a grid of molecular geometries, we now explain how the MORBID program system was used with those results to simulate the infrared spectra. The MORBID program system, which is used for triatomic molecules to calculate rovibrational term values, transition wavenumbers and spectral intensities, is discussed in detail in the original papers [28–32]; we refer the reader to these publications for more details. In order to implement the MORBID program system to calculate rovibrational term values, the following analytical expansion for the potential energy function must be used:

$$V(\Delta r_{12}, \Delta r_{32}, \bar{\rho}) = \sum_{jkl} G_{jkl} y_1^j y_3^k (1 - \cos\bar{\rho})^l \quad (2)$$

with

$$y_i = 1 - \exp(-a_i \Delta r_{i2}). \quad (3)$$

The quantity y_i in Eq. (3) is expressed in terms of the molecular constants a_i and the instantaneous internuclear distance displacements $\Delta r_{i2} = r_{i2} - r_{i2}^e$, i = 1 or 3, where r_{i2}^e is the equilibrium value of the distance r_{i2} between the "outer" calcium nucleus i = 1 or 3 and the "center" oxygen nucleus 2. As in Section 2, the quantity $\bar{\rho} = \pi - \angle$(Ca–O–Ca) and the G_{jkl} are expansion coefficients. For symmetrical molecules such as Ca_2O, we have $a_3 = a_1, r_{32}^e = r_{12}^e$, and $G_{jkl} = G_{kjl}$, so that the function $V(\Delta r_{12}, \Delta r_{32}, \bar{\rho})$ is invariant under the interchange of Δr_{12} and Δr_{32}. We determined the parameters r_{i2}^e, a_i and G_{jkl} in the potential functions for the $\tilde{X}$ and $\tilde{a}$ states in a least squares fitting to the *ab initio* points for each state, and the values obtained are listed in Table 1. The G_{jkl} parameters not given in this table were determined statistically to be insignificantly different from zero. The standard deviations of the fittings were 6.5 and 4.9 cm^{-1}, respectively, for the $\tilde{X}$ and $\tilde{a}$ states. The energy at the minimum of the $\tilde{X}$ state was determined to be −1435.039145 E_h and $T_e(\tilde{a})$ was obtained as 386.1 cm^{-1}.

At each molecular geometry considered in the *ab initio* calculation of the electronic energy, we have also calculated the components of the molecular dipole moment for the $\tilde{X}$ and $\tilde{a}$ states of CaOCa. These components are measured relative to the p and q axes defined in Fig. 1 of Ref. [29]. The pq axis system has the origin at the nuclear center of mass, and the p and q axes are in the plane defined by the three nuclei. The q axis bisects the bond angle ∠(Ca–O–Ca) and points so that the q coordinates of the "terminal" calcium nuclei 1 and 3 are positive. The p axis is perpendicular to the q axis and points so that the p coordinate of nucleus 3 is positive. The *ab initio* dipole moment components along the p and q axes are obtained as $\bar{\mu}_p = \langle\Psi_{elec}|\mu_p|\Psi_{elec}\rangle_{el}$ and $\bar{\mu}_q = \langle\Psi_{elec}|\mu_q|\Psi_{elec}\rangle_{el}$, respectively, where Ψ_{elec} is the electronic wavefunction of $\tilde{X}^1\Sigma_g^+$ or $\tilde{a}^3\Sigma_u^+$ CaOCa and the subscript 'el' indicates that integration is over the electronic coordinates only. These electronic matrix elements are expressed as parameterized functions of the nuclear coordinates, where the parameter values are obtained by fitting to the computed

ab initio values of the molecular dipole moments. For $\bar{\mu}_q$ and $\bar{\mu}_p$ we use the following analytical functions of the vibrational coordinates:

$$\bar{\mu}_q(\Delta r_{12}, \Delta r_{32}, \bar{\rho}) = \sin\bar{\rho}\sum_{jkl}\mu^{(q)}_{jkl}\Delta r^j_{12}\Delta r^k_{32}(1-\cos\bar{\rho})^l \quad (4)$$

and

$$\bar{\mu}_p(\Delta r_{12}, \Delta r_{32}, \bar{\rho}) = \sum_{jkl}\mu^{(p)}_{jkl}\Delta r^j_{12}\Delta r^k_{32}(1-\cos\bar{\rho})^l \quad (5)$$

where the $\mu^{(q)}_{jkl}$ and the $\mu^{(p)}_{jkl}$ are expansion coefficients.

In Eq. (4) we have $\mu^{(q)}_{jkl} = \mu^{(q)}_{kjl}$ so that the function $\bar{\mu}^{(q)}(\Delta r_1, \Delta r_3, \bar{\rho})$ is invariant under the interchange of Δr_{12} and Δr_{32}. Similarly, in Eq. (5) $\mu^{(p)}_{jkl} = -\mu^{(p)}_{kjl}$ and the function $\bar{\mu}_p(\Delta r_{12}, \Delta r_{32}, \bar{\rho})$ is antisymmetric under the interchange of Δr_{12} and Δr_{32}; in particular, $\mu^{(p)}_{jjl} = 0$.

We determine the parameters $\mu^{(q)}_{jkl}$ and $\mu^{(p)}_{jkl}$ by fitting Eqs. (4) and (5) to the *ab initio* dipole moment values. We used 10(7) parameters to fit 72(59) $\bar{\mu}_q$ values for the $\widetilde{X}(\tilde{a})$ state with a standard deviation of 0.0011(0.0060) D. We used 7(6) parameters to fit the 45(34) $\bar{\mu}_p$ values for the $\widetilde{X}(\tilde{a})$ state with a standard deviation of 0.0045(0.0019) D. In Table 2 we give the values obtained for the dipole moment parameters.

3.2. The term values and spectral simulations

We used the MORBID program system to calculate the rovibrational term values for the $\widetilde{X}$ and $\tilde{a}$ electronic states of $^{40}Ca^{16}O^{40}Ca$. The lower ($J = \ell_2$) rovibrational term values G_{vib} for the $\widetilde{X}$ and $\tilde{a}$ electronic states are given in Table 3 together with effective rotational constants B_{eff}. The values of G_{vib} and B_{eff} were obtained using the expression (for singlet states $N = J$)

$$E_{v,\ell_2}(N) = G_{vib} + B_{eff}[N(N+1) - \ell_2(\ell_2+1)] \quad (6)$$

for the two lowest MORBID-calculated term values in each vibrational state. For the $\tilde{a}$ electronic state, the effects of the non-zero electron spin were neglected.

The ^{44}Ca isotope has an abundance of 2% and, like ^{40}Ca, a nuclear spin of 0, and the ^{18}O isotope has an abundance of 0.2%. Thus, spectra of isotopologues involving ^{44}Ca and/or ^{18}O are very weak. However, as mentioned in Section 1, Andrews and Ault [4] carried out experiments involving ^{44}Ca and $^{18}O_3$, and so they attributed observed absorptions not only to $^{40}Ca_2{}^{16}O$, but also to $^{40}Ca_2{}^{18}O$ and $^{44}Ca_2{}^{16}O$. In order to generate theoretical predictions for comparison with all observed spectra, we have calculated with MORBID the term values of various isotopologues of Ca_2O, and the results are given in Table 4.

We have further used the MORBID program system to simulate the absorption spectra of $\widetilde{X}^1\Sigma^+_g$ and $\tilde{a}^3\Sigma^+_u$ $^{40}Ca^{16}O^{40}Ca$ in the wavenumber region 0–1500 cm^{-1}. The simulations were obtained separately for each electronic state for an absolute temperature $T = 15$ K and we included all states with J (N for the $\tilde{a}$ state) $\leqslant 20$. The results are given in Figs. 2 and 3. In these figures, each rotation–vibration transition is represented as a stick whose height is the integrated absorption coefficient $I(f \leftarrow i)$. The integrated absorption coefficient for an electric dipole transition from an initial state i (with energy E_i and rovibronic wavefunction ψ_i) to a final state f (with energy E_f and rovibronic wavefunction ψ_f) is given by [5]

$$I_{if} = \frac{8\pi^3 N_A \tilde{\nu}_{if}\exp\left(-\frac{E_i}{kT}\right)\left[1-\exp\left(-\frac{hc\tilde{\nu}_{if}}{kT}\right)\right]}{3hcQ} \times S(f \leftarrow i), \quad (7)$$

where the partition function

$$Q = \sum_w g_w \exp(-E_w/kT) \quad (8)$$

with the summation running over all rovibronic states of the molecule, $S(f \leftarrow i)$ is the line strength of an electric dipole transition

$$S(f \leftarrow i) = g_{ns}\sum_{m_i,m_f}\sum_{A=X,Y,Z}|\langle\psi_f|\mu_A|\psi_i\rangle|^2, \quad (9)$$

g_{ns} is the nuclear spin statistical weight, $\tilde{\nu}_{if} = (E_f - E_i)/(hc)$ is the transition wavenumber, g_w is the total degeneracy of the state with the energy E_w, (μ_X, μ_Y, μ_Z) are the components of the molecular dipole moment operator in the space-fixed XYZ axis system, N_A is the Avogadro constant, k is the Boltzmann constant, h is the Planck

Table 2
The electric dipole moment parameters of $\widetilde{X}^1\Sigma^+_g$ and $\tilde{a}^3\Sigma^+_u$ CaOCa obtained by fitting the analytical functions of Eqs. (4) and (5) through the calculated *ab initio* values.

		$\widetilde{X}^1\Sigma^+_g$	$\tilde{a}^3\Sigma^+_u$
$\bar{\mu}_p$	μ_{100}/D (Å^{-1})	−5.969(13)[a]	−6.4861(32)
	μ_{101}/D (Å^{-1})	9.23(20)	7.41(18)
	μ_{102}/D (Å^{-1})	9.58(88)	2.55(91)
	μ_{103}/D (Å^{-1})	4.24(97)	13.51(91)
	μ_{200}/D (Å^{-2})	−1.145(75)	−0.143(29)
	μ_{201}/D (Å^{-2})	−19.27(49)	−13.45(41)
	μ_{300}/D (Å^{-3})	2.99(70)	
$\bar{\mu}_q$	μ_{000}/D (Å)	−0.4758(16)	−0.3276(96)
	μ_{001}/D (Å)	−0.2183(60)	−0.139(48)
	μ_{002}/D (Å)		1.321(50)
	μ_{003}/D (Å)	1.5770(97)	
	μ_{100}/D (Å^{-1})	3.0811(74)	2.715(47)
	μ_{101}/D (Å^{-1})		−0.96(12)
	μ_{102}/D (Å^{-1})	−1.033(32)	
	μ_{200}/D (Å^{-2})	−2.873(99)	−1.25(48)
	μ_{201}/D (Å^{-2})	2.62(35)	
	μ_{110}/D (Å^{-2})	4.30(14)	3.05(73)
	μ_{111}/D (Å^{-2})	−2.35(51)	
	μ_{300}/D (Å^{-3})	3.72(55)	

[a] Quantities in parentheses are standard errors in units of the last digit given.

Table 3
The calculated vibrational term values $G_{vib} = E\left(v_1, v_2^{\ell_2}, v_3, N_{min} = \ell_2\right) - E(0, 0^0, 0, 0)$ and effective rotational constants B_{eff} (in cm^{-1}) for $^{40}Ca^{16}O^{40}Ca$ in the electronic states $\widetilde{X}^1\Sigma^+_g$ and $\tilde{a}^3\Sigma^+_u$.

$\left(v_1, v_2^{\ell_2}, v_3\right)$	N_{min}	$\widetilde{X}^1\Sigma^+_g$		$\tilde{a}^3\Sigma^+_u$	
		G_{vib}	B_{eff}	G_{vib}	B_{eff}
$(0,0^0,0)$	0	0.00[a]	0.0534	0.00[b]	0.0530
$(0,1^{1e},0)$	1	54.84	0.0538	82.71	0.0533
$(0,1^{1f},0)$	1	54.84	0.0539	82.71	0.0533
$(0,2^0,0)$	0	106.74	0.0545	163.73	0.0537
$(0,2^{2e,f},0)$	2	110.06	0.0545	166.39	0.0536
$(0,3^{1e},0)$	1	158.30	0.0549	244.22	0.0539
$(0,3^{1f},0)$	1	158.30	0.0552	244.22	0.0540
$(0,3^{3e,f},0)$	3	165.52	0.0550	250.96	0.0540
$(0,4^0,0)$	0	207.87	0.0557	324.59	0.0542
$(0,4^{2e,f},0)$	2	210.74	0.0556	327.01	0.0543
$(0,4^{4e,f},0)$	4	221.18	0.0556	336.49	0.0543
$(1,0^0,0)$	0	345.39	0.0533	344.54	0.0530
$(1,1^{1e},0)$	1	410.29	0.0536	435.59	0.0531
$(1,1^{1f},0)$	1	410.29	0.0537	435.59	0.0532
$(1,2^0,0)$	0	468.85	0.0543	520.38	0.0535
$(1,2^{2e,f},0)$	2	474.08	0.0542	525.73	0.0535
$(0,0^0,1)$	0	754.58	0.0531	755.92	0.0527
$(0,1^{1e},1)$	1	804.45	0.0536	834.68	0.0530
$(0,1^{1f},1)$	1	804.45	0.0537	834.68	0.0530
$(0,2^0,1)$	0	852.91	0.0543	914.71	0.0534
$(0,2^{2e,f},1)$	2	855.49	0.0543	915.89	0.0533
$(2,0^0,0)$	0	685.76	0.0537	681.76	0.0531
$(2,1^{1e},0)$	1	763.36	0.0535	788.34	0.0532
$(2,1^{1f},0)$	1	763.36	0.0536	788.34	0.0533
$(2,2^0,0)$	0	828.76	0.0541	875.90	0.0535
$(2,2^{2e,f},0)$	2	835.03	0.0539	884.43	0.0535

[a] Zero point energy is 606.1 cm^{-1}.
[b] Zero point energy is 633.6 cm^{-1}.

Table 4
Vibrational term values (in cm^{-1}) of various CaOCa isotopologues.

	$^{40}Ca^{18}O^{40}Ca$		$^{44}Ca^{16}O^{44}Ca$		$^{44}Ca^{18}O^{44}Ca$		$^{40}Ca^{16}O^{44}Ca$		$^{40}Ca^{18}O^{44}Ca$	
	$\tilde{X}$	$\tilde{a}$	$\tilde{X}$	$\tilde{a}$	$\tilde{X}$	$\tilde{a}$	$\tilde{X}$	$\tilde{a}$	$\tilde{X}$	$\tilde{a}$
ν_1	344	343	330	330	329	328	338	337	337	336
ν_2	52	79	55	82	52	78	55	82	52	78
ν_3	719	720	749	750	713	714	752	753	716	717
$2\nu_2$	102	156	106	162	101	155	106	163	102	155
$3\nu_2$	151	233	157	242	150	231	158	243	150	232
$\nu_1 + \nu_2$	405	429	395	420	390	414	403	428	397	421
$2\nu_1$	689	687	656	653	652	649	671	667	675	673
$2\nu_1 + \nu_2$	755	778	732	754	725	749	749	775	740	763

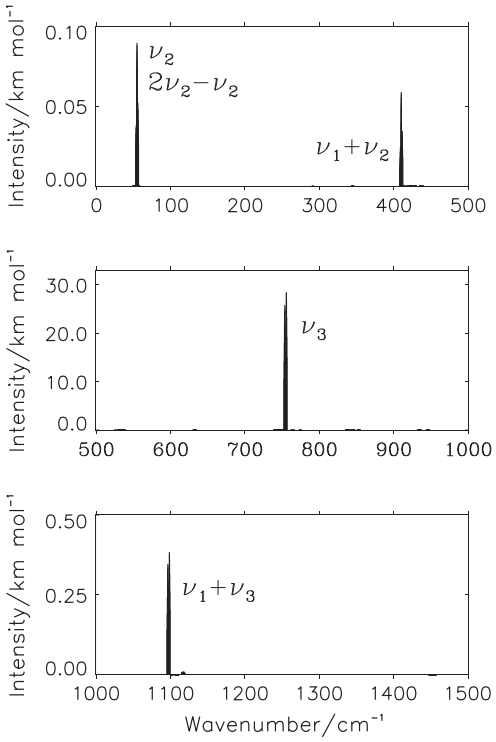

Fig. 2. The predicted infrared spectrum of $^{40}Ca^{16}O^{40}Ca$ in the $\tilde{X}^1\Sigma_g^+$ electronic state for $J \leqslant 20$ and $T = 15$ K in the wavenumber region below 1500 cm^{-1}. Note the very different ordinate scales on the three displays.

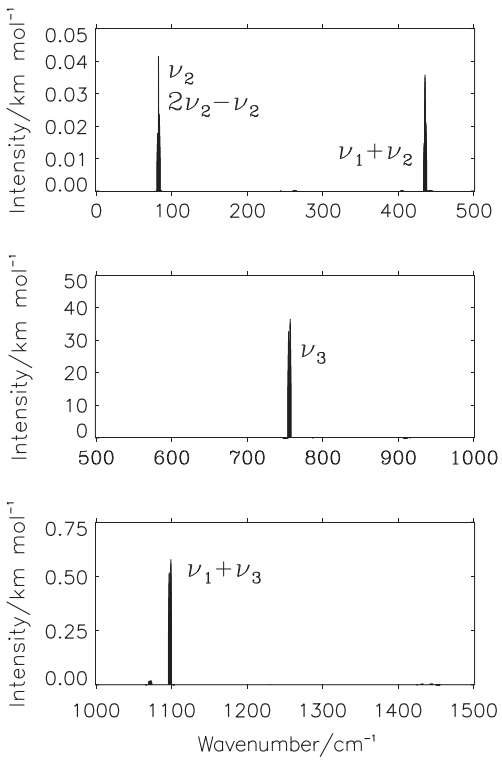

Fig. 3. The predicted infrared spectrum of $^{40}Ca^{16}O^{40}Ca$ in the $\tilde{a}^3\Sigma_u^+$ electronic state for $N \leqslant 20$ and $T = 15$ K in the wavenumber region below 1500 cm^{-1}. Note the very different ordinate scales on the three displays.

constant, and c is the speed of light in vacuum. In Eq. (9), m_i and m_f are the projections, in units of $\hbar = h/(2\pi)$, of the angular momentum onto the space-fixed Z axis in the initial and final states, respectively.

4. The $v = 1 \leftarrow 0$ band of CaO

It is useful to compare the predicted Ca_2O spectrum in the region of the ν_3 fundamental with an analogous simulation of the fundamental band of CaO. The simulation of the CaO fundamental band was kindly carried out by Prof. Le Roy [33] using his program LEVEL [34]. As input for LEVEL he used the CaO RKR potential energy curve derived from the $\tilde{X}$ state Dunham coefficients given in Table 2 of Ref. [35], and the *ab initio* dipole moment values determined by us and given in Table 5. We calculated the dipole moment at five internuclear distances: The RKR turning points for the $v = 2$ level (1.70 and 1.98 Å), the equilibrium bond length (1.82223 Å), and two intermediate points (1.761115 and 1.901115 Å).

Table 5
Dipole moment values calculated *ab initio* for the electronic ground state of CaO. The details of this *ab initio* calculation are given in the text.

r (Å)	μ (D)
1.700000	−8.75
1.761115	−9.21
1.822230	−9.57
1.901115	−9.89
1.980000	−9.99

For the *ab initio* calculation of the CaO dipole moment, the basis set employed for calcium and oxygen was cc-pCVQZ. At the CASSCF level of theory the closed orbital space contained 10 orbitals: 1σ-6σ and $1\pi - 2\pi$; the orbitals were restricted to be doubly occupied and optimized. The active orbital space included 7 orbitals: $7\sigma - 9\sigma$ and $3\pi - 4\pi$. At the MRCISD level, the closed orbitals composed of 1s, 2s, 2p, 3s and 3p AOs of Ca and 1s AO of O ($1\sigma - 6\sigma$ and $1\pi - 2\pi$) were doubly occupied but correlated through single

and double excitations while occupied orbitals (including closed) were $1\sigma - 9\sigma$ and $1\pi - 4\pi$. Relativistic effects were introduced through the DKH Hamiltonian. The dipole moments were obtained as the expectation values of the dipole moment operator at the MRCI level. In Ref. [10] an *ab initio* calculation of the dipole moment of CaO as a function of internuclear distance was made for several electronic states including the ground state. The results were presented in their Fig. 4. From that figure we can see that their results for the ground state are in close agreement to the results that we obtain here.

The output of LEVEL does not give the intensity of a rotation–vibration transition using the integrated absorption coefficient I_{if} (Eq. (7)) that we use here. Instead, using LEVEL, one calculates the Einstein coefficient for spontaneous emission A_{fi}. It is explained, for example, in Section 2.2 of Ref. [36] how A_{fi} is defined and how it is related to I_{if}. By combining Eq. (7) with Eq. (10) of Ref. [36] we obtain

$$I_{if} = \frac{N_A(2J_f+1)\exp\left(-\frac{E_i}{kT}\right)\left[1-\exp(-\frac{hc\tilde{\nu}_{if}}{kT})\right]}{8\pi c\tilde{\nu}_{if}^2 Q} \times A_{fi} \tag{10}$$

where J_f is the J value for the final (upper) state of the absorption transition considered and the other symbols have the same meaning as in Eq. (7). We calculate the partition function Q in the harmonic-oscillator/rigid-rotor approximation. Thus, $Q = Q_{\mathrm{vib}} \times Q_{\mathrm{rot}}$ with

$$Q_{\mathrm{vib}} = \sum_{v=0}^{\infty} \exp\left(-\frac{hcv\omega}{kT}\right) = \frac{1}{1-\exp\left(-\frac{hc\omega}{kT}\right)}, \tag{11}$$

ω being the harmonic vibrational wavenumber of CaO, and

$$Q_{\mathrm{rot}} = \sum_{J=0}^{\infty}(2J+1)\exp\left(-\frac{hcB_eJ(J+1)}{kT}\right), \tag{12}$$

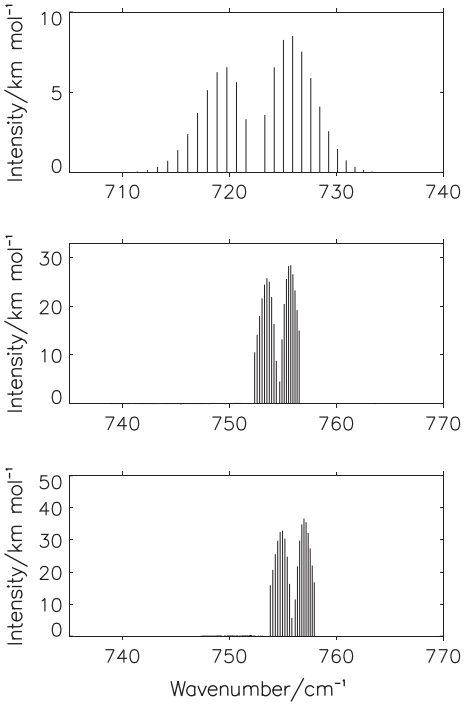

Fig. 4. Top panel: The predicted $v = 1 \leftarrow 0$ absorption band of $^{40}Ca^{16}O$ in the electronic ground state for $T = 15$ K. Middle and bottom panels: The predicted ν_3 band of $^{40}Ca^{16}O^{40}Ca$ in the $\widetilde{X}\,^1\Sigma_g^+$ and $\tilde{a}\,^3\Sigma_u^+$ electronic states, respectively, for $J \leqslant 20$ and $T = 15$ K. Note the different ordinate scales (and different wavenumber intervals) of the three displays.

where B_e is the rotational constant at the equilibrium geometry. We approximate $\omega = 722.3976\ \mathrm{cm}^{-1}$, the term value of the $J = 0$, $v = 1$ state of CaO determined experimentally by Blom and Hedderich [9] and calculate from Eq. (11) $Q_{\mathrm{vib}} = 1.000$ at $T = 15$ K. By approximating $B_e \approx B_0 = 0.44279641\ \mathrm{cm}^{-1}$ [9] and, for $T = 15$ K,

$$Q_{\mathrm{rot}} \approx \sum_{J=0}^{200}(2J+1)\exp\left(-\frac{hcB_0J(J+1)}{kT}\right), \tag{13}$$

we obtain $Q_{\mathrm{rot}} = 23.881$. Thus, at 15 K, $Q = Q_{\mathrm{vib}} \times Q_{\mathrm{rot}} = 23.881$. We are now in a position to use Eq. (10) to convert the A_{fi}-values calculated by Le Roy [33] to I_{if}-values for the $v = 1 \leftarrow 0$ band of CaO. The resulting simulated band is displayed in Fig. 4.

5. Summary and discussion

We report here *ab initio* calculations for the electronic ground state and the first excited electronic state of the Ca_2O molecule. The three-dimensional potential energy surface, and the electric dipole moment surfaces, have been calculated for each of the two electronic states by means of a multireference configuration interaction (MRCISD) approach in combination with internally contracted multireference perturbation theory (RS2C) based on full-valence complete active space self-consistent field (FV-CASSCF) wavefunctions with a cc-pwCVQZ-DK basis set for Ca and a cc-pCVQZ basis set for O. The electronic energy was calculated at 77 unique geometries for the electronic ground state and 59 unique geometries for first excited state; this characterizes each state to 1500 cm^{-1} above the respective minimum. We found that the $\widetilde{X}$ ground electronic state of Ca_2O has a linear, symmetrical CaOCa equilibrium structure with Ca–O bond length values of 1.995 Å. The symmetry of the $\widetilde{X}$ state electronic wavefunction is $^1\Sigma_g^+$. We have further found that the first excited electronic state is a very low lying triplet state, labeled $\tilde{a}$, of symmetry $^3\Sigma_u^+$. Also in this state, the CaOCa equilibrium structure is linear and symmetrical; the Ca–O equilibrium bond lengths are 1.998 Å. We determine that the singlet–triplet splitting, $T_e(\tilde{a})$, is 386 cm^{-1}.

We represent the surfaces as analytical functions and determine the values of the parameters in these functions by least squares fitting to the computed *ab initio* values. The parameters representing the potential energy surfaces are given in Table 1 and those representing the dipole moment surfaces in Table 2. Since these states have similar electronic structures, the parameters values characterizing the surfaces for the two states are in general very similar. Using the MORBID computer program system we have calculated rovibrational term values for both states and simulated their infrared absorption spectra for $^{40}Ca^{16}O^{40}Ca$. The vibrational term values, and effective B values, are given in Table 3, where again we see the similarity of the states. Also great similarity is seen between the simulated infrared spectra shown in Fig. 2 for the $\widetilde{X}$ state and in Fig. 3 for the $\tilde{a}$ state.

Just as we found for BeOBe [1] and MgOMg [2], for CaOCa the $\widetilde{X}$- and $\tilde{a}$-state bending potentials differ in a characteristic way: In the singlet $\widetilde{X}$ state, the bending potential increases less rapidly with the bond angle supplement $\bar{\rho} = 180^\circ - \angle(\mathrm{Ca–O–Ca})$ than in the triplet $\tilde{a}$ state. We can explain this difference in terms of, on one hand, the Walsh diagram [22] in Fig. 1 (which shows the $\bar{\rho}$-dependence of the orbital energies for the frontier orbitals involved in the leading configurations of the corresponding CI expansion) and in terms of, on the other hand, the $\bar{\rho}$-dependence of the CI coefficients. The energies of the highest occupied orbitals $11a_1$ and $9b_2$ (which correlate with $8\sigma_g$ and $7\sigma_u$, respectively, at linearity) are of particular interest; their orbital energies change very little as $\bar{\rho}$ varies from 0° to 50°. However, as the molecule bends further, the energy of the $11a_1$ orbital decreases and the energy of the $9b_2$ orbital increases. At linearity, the calculations involving solely

the $\widetilde{X}$ and $\tilde{a}$ states produced a CI wavefunction of 0.74 $|\ldots\ 11a_1^2\rangle - 0.60|\ldots\ 9b_2^2\rangle$ for the $\widetilde{X}$ state whereas for $\bar{\rho} = 70°$, this CI wavefunction has changed to 0.85 $|\ldots\ 11a_1^2\rangle - 0.40|\ldots\ 9b_2^2\rangle$. For the $\tilde{a}$ state, the composition of the CI wavefunction is largely independent of the bond angle; we obtain to a good approximation 0.95 $|\ldots\ 11a_1^1 9b_2^1\rangle$ for all $\bar{\rho}$-values between 0° and 70°. As $\bar{\rho}$ increases, the configuration involving $11a_1$ becomes increasingly dominant for the singlet state. As a consequence, the potential energy for the $\widetilde{X}$ state, in which the $11a_1$ orbital is doubly occupied, shows a less rapid increase as the molecule bends than the potential energy for the $\tilde{a}$ state, in which $11a_1$ and $9b_2$ orbitals are singly occupied.

We have shown here that the infrared spectrum of both the ground $\widetilde{X}$ electronic state and the excited $\tilde{a}$ electronic state of CaOCa is characterized by very strong ν_3 asymmetric CaO stretching fundamentals at around 755 cm^{-1} (Figs. 2 and 3). These bands have much greater intrinsic intensity than does the fundamental band of diatomic CaO at around 720 cm^{-1} (Fig. 4). Thus, we conclude that our results do not support the Ca_2O assignments made in Ref. [4] of the infrared spectrum resulting from the reaction products of Ca with O_2 or O_3, and it would seem that Ca_2O was not produced in those experiments. To further assist in characterizing the experimental infrared spectrum of Ca_2O, we also give the results of our calculations for the ^{44}Ca and ^{18}O isotopologues in Table 4.

In earlier papers we have made calculations for the BeOBe [1] and MgOMg [2] molecules similar to those of the present work. We found these two molecules to also have $\widetilde{X}^1\Sigma_g^+$ ground electronic states and low-lying $\tilde{a}^3\Sigma_u^+$ first excited electronic states. The singlet–triplet splittings were calculated to be 293 and 670 cm^{-1}, respectively, for BeOBe and MgOMg. It will be interesting to see what the situation is for the other members of this series: Sr_2O, Ba_2O and Ra_2O. We plan further *ab initio* studies on these three molecules.

Acknowledgements

We thank Professor Robert Le Roy both for using his program LEVEL to simulate the fundamental band of CaO so that we could present it in this work, and for giving the manuscript a critical reading. B.O. gratefully acknowledges the financial support of the Ministry of Science and Technological Development of Serbia (Contract No. 172001). P.S. is grateful to the Alexander von Humboldt Foundation for financial support and acknowledges support from the Marsden Fund (Wellington). A.G. acknowledges a stipend from the German Academic Exchange Service (DAAD) for a 6-month stay at Wuppertal. P.J. is grateful for support from the International Mobility Fund (Wellington) and the DAAD allowing him to visit Massey University Auckland. P.J. and P.R.B. are very grateful for hospitality at Massey University Auckland. The work of P.J. is supported in part by the Deutsche Forschungsgemeinschaft and the Fonds der Chemischen Industrie.

References

[1] B. Ostojić, P. Jensen, P. Schwerdtfeger, B. Assadollahzadeh, P.R. Bunker, J. Mol. Spectrosc. 263 (2010) 21–26.
[2] B. Ostojić, P.R. Bunker, P. Schwerdtfeger, B. Assadollahzadeh, P. Jensen, Phys. Chem. Chem. Phys. 13 (2011) 7546–7553.
[3] D.M. Thomas, L. Andrews, J. Mol. Spectrosc. 50 (1974) 220–234.
[4] L. Andrews, B.S. Ault, J. Mol. Spectrosc. 68 (1977) 114–121.
[5] P.R. Bunker, P. Jensen, Molecular Symmetry and Spectroscopy, second ed., NRC Research Press, Ottawa, 2006.
[6] L.v. Szentpaly, P. Schwerdtfeger, Chem. Phys. Lett. 170 (1990) 555–560.
[7] M. Hargittai, M. Kolonits, D. Knausz, I. Hargittai, J. Chem. Phys. 96 (1992) 8980–8985.
[8] K. Beloy, A.W. Hauser, A. Borschevsky, V.V. Flambaum, P. Schwerdtfeger, Phys. Rev. A 84 (2011) 062114/1–4.
[9] C.E. Blom, H.G. Hedderich, Chem. Phys. Lett. 145 (1988) 143–145.
[10] H. Khalil, V. Brites, F. Le Quéré, C. Léonard, Chem. Phys. 386 (2011) 50–55.
[11] H. Khalil, F. Le Quéré, V. Brites, C. Léonard, J. Mol. Spectrosc. 271 (2012) 1–9.
[12] H.-J. Werner, P.J. Knowles, J. Chem. Phys. 82 (1985) 5053–5063.
[13] P.J. Knowles, H.-J. Werner, Chem. Phys. Lett. 115 (1985) 259–267.
[14] H.-J. Werner, P.J. Knowles, J. Chem. Phys. 89 (1988) 5803–5814.
[15] P.J. Knowles, H.-J. Werner, Chem. Phys. Lett. 145 (1988) 514–522.
[16] P.J. Knowles, H.-J. Werner, Theor. Chim. Acta 84 (1992) 95–103.
[17] P. Celani, H.-J. Werner, J. Chem. Phys. 112 (2000) 5546–5557.
[18] J. Koput, K.A. Peterson, J. Phys. Chem. A 106 (2002) 9595–9599.
[19] D.E. Woon, T.H. Dunning Jr., J. Chem. Phys. 103 (1995) 4572–4585.
[20] D. Feller, J. Comp. Chem. 17 (1996) 1571–1586. <http://bse.pnl.gov/bse/portal>.
[21] H.-J. Werner, P.J. Knowles, R. Lindh, F.R. Manby, M. Schütz, P. Celani, T. Korona, G. Rauhut, R.D. Amos, A. Bernhardsson, A. Berning, D.L. Cooper, M.J.O. Deegan, A.J. Dobbyn, F. Eckert, C. Hampel, G. Hetzer, A.W. Lloyd, S.J. McNicholas, W. Meyer, M.E. Mura, A. Nicklass, P. Palmieri, R. Pitzer, U. Schumann, H. Stoll, A.J. Stone, R. Tarroni, T. Thorsteinsson, MOLPRO, Version 2008.1, A Package of Ab Initio Programs. <http://www.molpro.net>.
[22] P.R. Bunker, P. Jensen, Fundamentals of Molecular Symmetry, IOP Publishing Ltd., Bristol UK and Philadelphia, 2005. pp. 196–197. <http://www.crcpress.com/shopping_cart/products/product_detail.asp?sku=IP298>.
[23] S.R. Langhoff, E.R. Davidson, Int. J. Quant. Chem. 8 (1974) 61–72.
[24] I.S. Lim, H. Stoll, P. Schwerdtfeger, J. Chem. Phys. 124 (2006) 034107/1–9.
[25] M. Reiher, A. Wolf, J. Chem. Phys. 121 (2004) 2037–2047.
[26] M. Reiher, A. Wolf, J. Chem. Phys. 121 (2004) 10945–10956.
[27] A. Wolf, M. Reiher, B.A. Hess, J. Chem. Phys. 117 (2002) 9215–9226.
[28] P. Jensen, J. Mol. Spectrosc. 128 (1988) 478–501.
[29] P. Jensen, J. Mol. Spectrosc. 132 (1988) 429–457.
[30] P. Jensen, J. Chem. Soc. Faraday Trans. 84 (2) (1988) 1315–1340.
[31] P. Jensen, in: S. Wilson, G.H.F. Diercksen (Eds.), Methods in Computational Molecular Physics, Plenum Press, New York, 1992.
[32] P. Jensen, in: U.G. Jørgensen (Ed.), Molecules in the Stellar Environment, Lecture Notes in Physics, vol. 428, Springer-Verlag, Berlin, 1994.
[33] R.J. Le Roy, private communication, 2011.
[34] R.J. Le Roy, Level 8.0: A Computer Program for Solving the Radial Schrödinger Equation for Bound and Quasibound Levels, University of Waterloo Chemical Physics Research Report CP-663 (2007); <http://leroy.uwaterloo.ca/programs/>.
[35] C. Focsa, A. Pocleta, B. Pinchemela, R.J. Le Roy, P.F. Bernath, J. Mol. Spectrosc. 203 (2000) 330–338.
[36] S.N. Yurchenko, W. Thiel, M. Carvajal, H. Lin, P. Jensen, Adv. Quant. Chem. 48 (2005) 209–238.